Ocean Sci. Discuss., https://doi.org/10.5194/os-2018-113
Manuscript under review for journal Ocean Sci.
Discussion started: 22 October 2018

Ocean Science Discussions

Data assimilation of SMOS observations into the Mercator Ocean operational system: focus on the Nino 2015 event

Benoît Tranchant[1], Elisabeth Remy[2], Eric Greiner[1] and Olivier Legalloudec[2]

[1]Collecte Localisation Satellites, Ramonville Saint-Agne, 31520, France
[2]Mercator-Océan, Ramonville Saint-Agne, 31520, France

Correspondence to: Benoît Tranchant (btranchant@groupcls.com)

Abstract. Monitoring **S**ea **S**urface **S**alinity (SSS) is important for understanding and forecasting the ocean circulation. It is even crucial in the context of the acceleration of the water cycle. Until recently, SSS was one of the less observed essential ocean variables. Only sparse in situ observations, most often closer to 5 meters deep than the surface, were available to estimate the SSS. The recent satellite missions of ESA's SMOS, NASA's Aquarius, and now SMAP have made possible for the first time to measure SSS from space.

The SSS drivers can be quite different than the temperature ones. The model SSS can suffer from significant errors coming not only from the ocean dynamical model but also the atmospheric precipitation and evaporation as well as ice melting and river runoff. Satellite SSS can bring a valuable additional constraint to control the model salinity.

In the framework of the SMOS Nino 2015 ESA project (https://www.godae-oceanview.org/projects/smos-nino15/), the impact of satellite SSS data assimilation is assessed with the Met Office and Mercator Ocean global ocean analysis and forecasting systems with a focus on the Tropical Pacific region. This article presents the analysis of an Observing System Experiment (OSE) conducted with the ¼° resolution Mercator Ocean analysis and forecasting system. SSS data assimilation constrains the model SSS to be closer to the observations in a coherent way with the other data sets already routinely assimilated in an operational context. Globally, the SMOS SSS assimilation has a positive impact in salinity over the top 30 meters. Comparisons to independent data sets show a small but positive impact. The sea surface height (SSH) has also been impacted by implying a reinforcement of TIWs during the El-Niño 2015/16 event. Finally, this study helped us to progress in the understanding of the biases and errors that can degrade the SMOS SSS performance.

1 Introduction

Thanks to progress in data treatment, SSS observations (SMOS, Aquarius and SMAP) from space have now a good accuracy so they can be assimilated in ocean analysis systems (Boutin et al., 2017). Here we present the impact of assimilating SSS observations from space into the global ¼° Mercator Ocean operational system. The changes induced by the satellite SSS data assimilation, considering all of the other ocean observing components, are analyzed. The focus has been primarily on the 2015-2016 El Niño event in the Tropical Pacific associated with strong SSS anomalies, seen in in both model and observations (Hasson et al., 2018; Gasparin and Roemmich, 2016; Guimbard et al., 2017). The salinity plays an important role in the ocean-

atmosphere coupling in this region by isolating the ocean interior due to the formation of a Barrier Layer. It is then not only the thermocline depth that is of importance but also the halocline when it becomes shallower than the thermocline.

The most striking event in the global ocean for the year 2015 was the strong El Nino event. When considering its intensity in terms of SST anomaly (ENSO index), it is as strong as the 1997 one, see section 2.6 in (Von Schuckmann et al., 2018). Looking at the more recently used Multivariate ENSO Index (MEI) that takes into account other surface ocean and atmosphere variables, it appears less intense but its onset in 2014 is visible. It was more a Modoki El Nino (Ashok and Yamagata, 2009) than a « classical » one. The maximum of the SST anomalies stays off the eastern coast of South and Central America.

Warm anomalies began to build in the western pacific in 2014 triggered by Westerly Wind Bursts but did not lead to the development of an El Nino. Only in 2015 did they lead to an El Nino event. As shown in (Corbett et al., 2017), both periods are characterized by strong Westerly Wind Events (WWEs) in January–March, but no subsequent WWEs occurred from April to July 2014 while there were WWEs in April and June 2015. The 2015 El Niño included a reduction in Pacific trade winds with anomalous cross equatorial southerly surface winds in the eastern Pacific and an eastward shift in the ITCZ. El Niño contributed to record high global average SSTs in 2015. It was anomalously warm from the dateline all the way to South America along the equator. Anomalously eastward currents along the equator and in the NECC continued a pattern from 2014. These anomalous currents contributed to sea level and upper ocean heat content (OHC) falling in the western tropical Pacific and rising in the east, again building on the 2014 pattern. This is associated with an increase in precipitation and an eastward shift in fresh surface salinities. A strong equatorial SSS anomaly in 2015 has been observed and described, see for example (Hasson et al., 2018; Gasparin and Roemmich, 2016). The Pacific freshening is due to a strong ITCZ in 2015, but advection by anomalous eastward currents also plays a role in the SSS changes. Moreover, as suggested by (McPhaden et al., 2015), the presence of El Niño precursors in early-2014 helped the development of a strong El Niño at the end of 2015. The difference of the two annual anomalies in 2014 and 2015 in our control run (see section 2.4) is shown in Fig. 1. The 2015–2016 El Niño is also the first important climatic event fully captured by the SMOS satellite where negative SSS anomalies have been observed between 0 and 15°N around 170°W from mid-2014 to mid-2015 (Boutin et al., 2016). Note that recently, significant freshening was also observed around 20°N, (Hasson et al., 2018).

Data assimilation experiments conducted within the SMOS Nino 2015 project (https://www.godae-oceanview.org/projects/smos-Niño15) are helping to prepare the assimilation of space SSS data and allow testing their impact on short term ocean forecast and analysis. To evaluate the impact of SSS observations from satellites on ocean monitoring and forecast systems in a realistic context, Observing System Experiments (OSE) were conducted with the UK Met Office and Mercator Ocean global ocean forecast systems. The OSE approach consists of comparing two identical assimilation experiments except that one data set, here the satellite SSS, is withheld from the analysis in one of the experiments. The differences between the two simulations highlight the "impact" of the withheld observations. SST, SLA and in situ observations are assimilated as currently done in the operational systems, see (Martin et al., 2018). This is a commonly agreed approach to evaluate observation networks within the GODAE OceanView community (Oke et al., 2015, Lea et al., 2014).

The assimilation of satellite SSS observations is challenging because of the various and complex biases that affect them, see (Köhl et al, 2014). The difference between the forecast and the satellite SSS can be 5 times larger than the misfit between the forecast and near surface ARGO salinity. The signal to noise ratio is still not high today, and data and methods must be improved. Nevertheless, several studies (Reul et al., 2013 or Lee et al., 2012) show that SSS measured from space can bring new information. Recently, (Toyoda et al., 2014; Hackert et al., 2014) show the impact of assimilating Aquarius data in the Pacific region both in uncoupled and coupled ocean-atmosphere systems. In a recent paper, (Chakraborty et al., 2014) show that the migration of the thermohaline fronts at the eastern edge of the western Pacific warm pool can be more realistic with the assimilation of Aquarius SSS. Data assimilation of Aquarius SSS can also help to better understand the variability of salinity structure in the Bay of Bengal (BoB) (Seelanki et al., 2018). Finally, SSS assimilation from space is still promising in an operational context both for ocean and seasonal forecasting.

Nevertheless, technical challenges are still open to assimilate SSS data efficiently in the context of global ocean analysis and forecasting. Careful analysis of the SSS data sets shows that a bias correction is needed before their assimilation. To have an optimal analysis, the hypothesis of unbiased errors has to be respected. This article details the bias correction scheme and the error estimation scheme used in the data assimilation system for those data. This was a necessary step to have a positive impact of SSS data assimilation.

Experiments conducted within the SMOS Nino15 project to test the impact of the satellite SSS data were carefully designed and analyzed to ensure robust conclusions on the impact of SSS measurements on ocean analysis. The system used for the OSE is based on the operational ocean monitoring and forecasting system operated at Mercator Ocean. The use of such system ensures that conclusions are relevant for such operational applications.

To assess the benefit of assimilating SSS from satellite in a realistic context, all observations from the Global Ocean Observing System (GOOS) that are assimilated in real time ocean analysis or reanalysis are also assimilated. SST, in situ temperature and salinity observations (from moorings, drifting platforms, ships) and along track Sea Level Anomalies in the so-called Reference simulation are assimilated (hereafter REF). OSEs conducted were designed to assess the impact of weekly products as the system has a weekly assimilation cycle.

It is recommended to withhold part of the usually assimilated observations from the OSE experiments to have fully independent data to compare with, see Lahoz et al., 2010. The TAO mooring salinity data were not assimilated and kept for verification. Even if restricted to the few mooring points, those data are the only ones to provide long term time series of daily temperature and salinity observations.

The structure of this article is as follows: after a description of the system and the presentation of the experimental design in section 2, the effects of the SMOS data assimilation are discussed in section 3, while discussions and conclusions are provided in section 4.

Ocean Sci. Discuss., https://doi.org/10.5194/os-2018-113
Manuscript under review for journal Ocean Sci.
Discussion started: 22 October 2018

2. System description

The OSE are conducted with the global ¼° ocean analysis and forecasting system running in real time at Mercator Ocean. Detailed descriptions of the system can be found in (Lellouche et al., 2013; Lellouche et al., 2018). After a brief description of the system configuration, we will describe in more detail the data assimilation components that were specifically developed or adapted for the SSS data assimilation.

2.1 Ocean model and configuration

The Mercator Ocean real time analysis and forecast is based on the version 3.1 of the NEMO ocean model (Madec, 2016), which uses a ¼° ORCA grid. The water column is discretized into 50 vertical levels, including 22 levels within the upper 100 m, with 1-m resolution at the surface to 450-m resolution at the bottom. The system has been initialized in autumn 2006, using temperature and salinity profiles from the EN4 climatology (Good et al., 2013).

The ocean model is forced by atmospheric fields from the European Centre for Medium-Range Weather Forecasts-Integrated Forecast System (ECMWF-IFS) at 3-hr resolution to reproduce the diurnal cycle. Momentum and heat turbulent surface fluxes are computed by using (Large and Yeager 2009) bulk formulae. Due to large known biases in precipitation, a satellite-based large-scale correction of precipitation has been performed with climatological estimates from GPCPV2.1 rain-fall (Lellouche et al., 2013) and applied to the precipitation fluxes.

A monthly river runoff climatology is built with data on coastal runoff and 100 major rivers from the Dai et al. (2009) database instead of Dai and Trenberth (2002). This database uses new data, mostly from recent years, streamflow simulated by the Community Land Model version 3 (CLM3) to fill the gaps, in all lands areas except Antarctica and Greenland. At high latitude the effect of iceberg melting is also parameterized. The lack of interannual variability of the largest rivers is known to lead to large errors in the surface ocean salinity in the analysis and forecast. There is no SSS relaxation term to any climatology like in the operational case. More details concerning parameterization of the terms included in the momentum, heat and freshwater balances (i.e, advection, diffusion, mixing and surface fluxes) can be found in (Lellouche et al., 2018).

2.2 Assimilated Observations

2.2.1 Current Network

All ocean observations assimilated in the real time forecasting system are assimilated in the same way in the OSEs presented here. Along track SLA observations distributed by CMEMS (http://marine.copernicus.eu/) referenced to an unbiased Mean Dynamic Topography (MDT) based on the CNES/CLS 2013 MDT are used. Gridded satellite SST observations (L4) from the OSTIA analysis are assimilated each week in addition to SST measurements from the in situ database delivered by the CORIOLIS centre (http://www.coriolis.eu.org/). Assimilation of in situ temperature and salinity profiles from this database are from Argo floats, XBT, CTDs, moorings, gliders and sea mammals. The assimilation of those routine observations in the OSEs provides a realistic context for the global ocean observing system so that the experiments address the complementarity

of the different data sets with satellite SSS. The only exception is the TAO mooring observations of salinity that are withheld from the analysis and kept as independent observations to evaluate the performance of the assimilation experiment and the impact of the SSS assimilation. The SSS in the real time system is only constrained at large scale by in-situ observations, mostly Argo floats that usually start to measure at 5 meters depth.

2.2.2 SSS from space

In this study, we assimilate a SMOS L3 gridded SSS product at 0.25° resolution. L3 products are qualified (quality controlled) and processed at the Data Production Center (CPDC) of the Centre Aval de Traitement des Données SMOS (CATDS CEC-LOCEAN) (Boutin et al., 2017). Compared to L2 products they benefit from additional corrections. These are 18-day products sampled at 25km resolution provided every 4 days (the precise description of the time filtering is in the documentation at http://www.catds.fr/Products/Available-products-from-CEC-OS/L3-Debiased-Locean-v2). We have checked that this temporal resolution fits well the model resolution and the weekly analysis window. In practice, the gridded SSS which is the closest to the analysis date (the fourth day of the week) provides the SSS data for the cycle. The model counterpart is the time average over the cycle. Due to a low signal to noise ratio, the assimilation of the SSS data is limited in the latitudinal band between 40°S and 40°N.

2.3 Data Assimilation Scheme

The assimilation scheme implemented in the real time Mercator Ocean systems is based on a reduced order Kalman Filter called SAM2 (Système d'Assimilation Mercator V2) and a 3DVar bias correction for large scale 3D temperature and salinity fields. Both are described in (Lellouche et al., 2013; Lellouche et al., 2018).

2.3.1 Background Error Covariances

The SAM2 system uses a background error covariance matrix based on a reduced basis of multivariate model anomalies built from a fixed collection of model anomalies. The anomalies are computed from a previous simulation for a period of 8 years with the in-situ bias correction, detailed in the section 2.3.3. The forecast error covariances rely on a fixed basis, seasonally variable ensemble of anomalies calculated from this long experiment. A significant number of anomalies are kept from one analysis to the other, thus ensuring error covariance continuity. The aim is to obtain an ensemble of anomalies representative of the error covariance (Oke et al., 2008), which provide an estimate of the error on the ocean state at a given period of the year. The localization of the error covariance is performed assuming a zero-covariance beyond a distance defined as twice the local spatial correlation scale. These spatial correlation scales are also used to select the data around the analysis point. The model correction (analysis increment) is a linear combination of these anomalies. This correction is applied progressively over the assimilation cycle temporal window using an incremental analysis update, see Bloom et al., 1996; Benkiran and Greiner 2008).

Ocean Sci. Discuss., https://doi.org/10.5194/os-2018-113
Manuscript under review for journal Ocean Sci.
Discussion started: 22 October 2018

2.3.2 Observation Error Covariances

The observation errors specified in the assimilation scheme are assumed to be uncorrelated with each other. Observation errors include representativity errors specified as a fixed error map and an instrumental error. The instrumental errors of SLA, SST and in situ measurements are summarized in Table 1. Fig. 2 shows the representativity error used for the in-situ SSS and Fig. 3 shows an example of the resulting salinity error for in-situ data for the week 20-27 January 2016.

2.3.3 Bias correction scheme

A bias correction based on variational methods (3D-Var) is applied to the model's prognostic equations to correct large scale and slowly evolving (1 month - 1°x1°) errors in T and S diagnosed from the in-situ profile innovations over the preceding month. The bias is the minimum of the cost function given by the Eq. 1a, where $\boldsymbol{x}$ is the in-situ bias to estimate, **B** is the background error covariance of the 3D bias, d is the innovation vector (it is the mean innovation over 1 month on a 1°x1° grid between 0 and 10 meters depth and the mean is symbolized by <>), **H** is the observation operator, **R** is the observation covariance error. Eq. 1b corresponds to the extra terms to take into account biases in the satellite SSS data.

Because temperature and salinity biases are not necessarily correlated, these two variables are processed separately. Spatial correlations in **B** are modeled by means of an anisotropic Gaussian recursive filter. Finally, bias correction of T, S and dynamic height are computed and interpolated on the model grid and applied as tendencies in the model prognostic equations with a 1-month time scale.

$$J(\boldsymbol{x},\boldsymbol{\xi}) = {}^1\!/_2\, \boldsymbol{x}^{\boldsymbol{T}}\, \mathbf{B}^{-1}\boldsymbol{x} + {}^1\!/_2\, (\mathrm{d}\text{-}\mathbf{H}\,\boldsymbol{x})^{\boldsymbol{T}}\mathbf{R}^{-1}(\mathrm{d}\text{-}\mathbf{H}\,\boldsymbol{x}) \quad (\mathbf{1a})$$

$$+ {}^1\!/_2\, \boldsymbol{\xi}^{\boldsymbol{T}}\boldsymbol{B}_{\xi}^{-1}\boldsymbol{\xi} + {}^1\!/_2\, \left(\boldsymbol{d}_{\xi} - \mathbf{H}\,\boldsymbol{\xi}\right)^{\boldsymbol{T}}\boldsymbol{R}_{\xi}^{-1}\left(\boldsymbol{d}_{\xi} - \mathbf{H}\,\boldsymbol{\xi}\right) \quad (\mathbf{1b})$$

where

$$d = \langle \mathbf{SSS}_{\boldsymbol{in-situ}} \rangle - \langle \mathbf{SSS}_{\boldsymbol{model(0.5-10m)}} \rangle \text{ and } \boldsymbol{d}_{\xi} = (\langle \mathbf{SSS}_{\boldsymbol{SMOS}} \rangle - \boldsymbol{\xi}^{\boldsymbol{T}}) - \langle \mathbf{SSS}_{\boldsymbol{model(0.5m)}} \rangle$$

Earlier attempts to assimilate SSS data have shown the importance of using unbiased satellite SSS data while implementing rigorous quality control in an upstream process (Tranchant et al., 2015). In this study, the bias control of satellite SSS has been modelled by modifying the current T/S bias (in-situ) correction 3Dvar cost function (Eq. 1a). A new control term for SSS has been added, denoted $\boldsymbol{\xi}$ in the 3DVar cost function (Eq.1b) where $\boldsymbol{d}_{\xi}$ is the innovation of SSS bias at surface, see eq. 2. To get an optimal set of parameters (weights, spatial scales and errors), several estimations were performed with data withdrawing. In Fig. 4, examples of model salinity bias near the surface ($\boldsymbol{x}$) with and without the SSS bias term ($\boldsymbol{\xi}$) are shown. The patterns are similar except at the equator. They have different magnitude due to the addition of the SSS bias. The Fig. 4 shows the SSS bias ($\boldsymbol{\xi}$ term of the Eq. 1). The patterns are different than the model bias (Fig. 4) and often of opposite sign but have the same magnitude. The SSS bias from SMOSexp have smaller scales than the model bias.

Ocean Sci. Discuss., https://doi.org/10.5194/os-2018-113
Manuscript under review for journal Ocean Sci.
Discussion started: 22 October 2018

2.3.4 SSS observation error

The Desroziers Diagnostic (Desroziers et al., 2005) is commonly used for estimating observation error statistics and is used here to adapt the observation error from the background and analysis residuals calculated in the bias correction, see also (Lellouche et al., 2018). Following (Desroziers et al., 2005), the observation error of the bias $\boldsymbol{R_\xi}$ is optimal when equal to the statistical expectation of the cross-product between the residual $\boldsymbol{d_\xi^a}$ and the innovation $\boldsymbol{d_\xi}$ of the SSS bias, see Eq. 2.

$$\boldsymbol{R_\xi} = \boldsymbol{E}\,[\boldsymbol{d_\xi}.\boldsymbol{d_\xi^a}] \quad \textbf{(2)}$$

Actually, $\boldsymbol{R_\xi}$ is estimated iteratively (n=5) by an iterative boot-strap method computed on a 3°x3° grid from an observation error a priori $\boldsymbol{R_\xi^o}$ and by the successive ratio $\boldsymbol{r_\xi^{i=1,n}}$, see Eq. 3:

$$\boldsymbol{R_\xi} = \boldsymbol{r_\xi^1} \ldots \boldsymbol{r_\xi^n}\ \boldsymbol{R_\xi^o} \quad \boldsymbol{with}\ \boldsymbol{r_\xi^{i=1,n}} = \frac{\boldsymbol{E}\,[\boldsymbol{d_\xi}.\boldsymbol{d_\xi^a}]}{\boldsymbol{R_\xi^{i=1,n}}} \quad \textbf{(3)}$$

The a priori error $\boldsymbol{R_\xi^o}$ is a combination of a zonally varying error, together with an increase over regions with sparse in-situ data. This increase varies with the cycle. It means that the SSS bias could not be estimated accurately in the absence of in situ data, and hence will have no impact in the assimilation in those regions void of in situ data. Fig. 6 illustrates how the fixed zonal error is increased near the equator. It is also reinforced near central America where in situ data are sparse. There is a local increase near Samoa (170°W-13°S), probably due to RFI pollution.

Finally, for each weekly analysis, the total observation error of satellite SSSS (SMOS) prescribed in the data assimilation scheme is the maximum of the above observation error estimated during the bias correction process and the measurements error ($\boldsymbol{R_{instr.}}$) supplied by the data producers (used as a threshold) , see Eq. 4. These measurement error estimates bring smaller scales than can be estimated by the Desroziers diagnostic.

$$\boldsymbol{R_{Tot}} = \boldsymbol{max}(\boldsymbol{R_\xi}\ , \boldsymbol{R_{instr.}}) \quad \textbf{(4)}$$

2.4 OSEs experiment design

Two parallel simulations were produced, the REF experiment and the SMOS experiment (hereafter SMOSexp) see Table 2. The only difference is the assimilation of the SSS SMOS observations. Both experiments begin in January 2014 from the same initial conditions coming from a previous reanalysis using only the bias correction of T/S without any data assimilation. The period covers the onset and development of the El-Nino 2015 event. The length of the OSE should at least cover one year, more if possible, as it takes 3 months for the system to be in equilibrium with the new data assimilated. This "adjustment" period is longer for observations deeper in the ocean (below the thermocline). Here, up to 2-year simulations are analyzed (2014-March2016).

The comparison between the two simulations highlights the impact of the SSS data assimilation on the ocean circulation and the comparison to the other observations (independent or not) will allow us to verify the coherency between the different observation networks and the way they are assimilated.

Ocean Sci. Discuss., https://doi.org/10.5194/os-2018-113
Manuscript under review for journal Ocean Sci.
Discussion started: 22 October 2018

3. OSE experiment analysis

Different diagnostics are now used to assess the impact of SSS data assimilation on the analysed model fields. First the analysis from the REF and SMOSexp simulations are evaluated against the assimilated observations. Then, the 3D fields of the simulations with and without SSS data assimilated are compared and the changes in the surface and subsurface fields are analysed. Finally, TOA/Triton array salinity observations which are deliberately with-held and delayed time ThermoSalinoGraph (TSG) which are not assimilated in the analysis of all experiments are used to conduct independent analysis observation comparison. The analysis focuses on the tropical Pacific region during the Niño 2015 event.

3.1 Evaluation of the analysis toward assimilated observations

3.1.1 Assimilation diagnostics

The REF and SMOSexp simulations differ only by the SSS data set assimilated (Table 2). We first check the success of the assimilation procedure in reducing the misfit between the assimilated SSS observations within the prescribed error bar. We then look at the in-situ salinity observation innovations near 5 meters depth, assimilated in both simulations. The model forecast range used in this comparison is from 1 to 7 days.

Fig. 8 shows the time-series of Root-Mean-Square Error (RMSE) between the model near-surface salinity compared to in situ observations (dotted lines) and the bias-corrected SMOS SSS (solid lines) for both simulations (REF in black, SMOSexp in red). As expected, the SMOS SSS data assimilation clearly leads to a significant reduction in the innovations of the SMOS data. Global, Tropical Pacific and central Pacific (Nino3.4) regional statistics are shown. The global RMSE to SMOS data is around 0.28PSS in the reference simulation and reduced to 0.21PSS when SMOS data are assimilated, corresponding to an error reduction of 24%. The innovation of the in-situ salinity observations is also slightly reduced by 5%. This shows that the assimilation of SMOS SSS observations do not introduce overall incoherent information and reduce the misfit to the in-situ observations. It also confirms that errors in the assimilation scheme are well tuned and the data bring coherent information (biases are removed well). Similar results are found for all the Tropical regions with a SMOS SSS RMSE reduction of 25%, and an in-situ salinity RMSE reduction of 5%, see Table 3. It should be mentioned that the number of in situ salinity observation per week is not always sufficient to ensure robust statistics in small regions.

Time series and maps of the misfits between observation and model forecasts are complementary to analyse the temporal and spatial variability of the model observation differences. Fig. 9 shows the mean and standard deviation of the daily ?? or monthly differences between the (analyzed) SSS for REF and SMOSexp simulations compared to the SMOS SSS observations (non-debiased). Statistics are computed over the year 2015 for the Tropical Pacific Ocean.

As expected, this comparison shows that both the mean and the standard deviation of the SSS errors are significantly reduced by the data assimilation of SMOS SSS. The mean SSS bias exhibits large scale patterns, coinciding with the 2015 SSS anomaly for the open ocean (Fig. 1). The largest mean differences are found close to the coast, in the Indonesian Archipelago and in the equatorial Pacific. The highest error standard deviations are also found close to the coast, in the Indonesian Archipelago and

in the eastern freshwater pool and in the region of the Inter Tropical Convergence Zone and SPCZ. The standard deviation is reduced to less than 0.2PSS (black isohaline on Fig. 9) in most of the Tropical Pacific Ocean.

Assimilation of surface salinity observations from satellite has a slight impact on subsurface salinity fields. The mean RMSE and the percentage of RMSE difference of the salinity profiles (mainly from Argo floats) are computed over the entire period and the global domain (Fig. 10). There is a slight decrease in the first 20 meters below the surface when SSS data are assimilated additionally to in situ salinity data. It shows that the additional information brought by the SSS is in agreement with the salinity in situ observation close to the surface. It can even help improving the global salinity representation in the first 20 meters by better constraining the model forecast with the satellite SSS.

In situ temperature innovations in the global domain as well as in the Tropical Pacific region do not show significant changes. The same is found for SLA (SALTO/DUACS along track) and SST innovations (OSTIA L4). SSS data assimilation has a neutral impact on the innovations associated with those observations.

3.1.1 Impact of assimilating SMOS data during El-Niño 2015/16

We now look at the changes in the analysed surface and subsurface fields due to the SSS data assimilation by comparing the 3D analysis of the REF and SMOSexp experiments. At basin scale, the REF simulation already agrees well with the 2015 mean deduced from the "unbiased" CATDS SMOS observations (Fig. 11)**.** SMOS data assimilation induced changes in the order of 0.2PSU. It tends to weaken the salinity negative anomaly represented in the REF simulation within the ITCZ and SPCZ regions. This is in agreement with (Kidd et al., 2013) that show an overestimation of the ECMWF precipitation in the tropics compared to satellite observations. Elsewhere, the SMOS data assimilation increases the salinity. Large changes also occurred in the coastal zones (Indonesian archipelago and Central America coast), even if the specified error on SSS data was larger in those regions than in the open ocean.

The associated vertical salinity changes to the SMOS SSS data assimilation at the equator are represented on Fig. 12. The largest magnitudes (saltier) are found in the first 50 m depth and along the coastal bathymetry, elsewhere changes are very small, less than 0.05 PSU. Overall, at the equator (excepted in coastal areas), the data assimilation of SMOS SSS leads to fresher waters in the East and saltier waters in the West for the year 2015.

The highest variability of the surface salinity at monthly scale during the year 2015 is found within the ITCZ, SPCZ and in the Eastern Pacific fresh pool, in both simulations and SMOS observations (not shown). SMOS assimilation decreases the intensity of the variability of the SSS, in agreement with the observed variability. In summary, the SSS assimilation acts to counteract the precipitation excess, with a visible result on the salinity both in terms of time mean but also in term of variability. During the Nino2015 event, a strong salinity anomaly pattern developed in the Tropical Pacific (Gasparin et Roemmich 2016). This anomaly corresponds to the ITCZ and SPCZ locations. Fig. 13 shows the evolution of the SSS at 5°N, the latitude where the salinity anomaly is the largest (Hackert et al., 2014). Both the REF and SMOSexp simulations represent the decrease in time of the salinity peaking in fall 2015 at this latitude, for the longitude between 160°E and 120°W. Note that this salinity

anomaly is lower in the SMOS data (SMOS SSS is salter) with a smaller extent. The Eastern freshwater pool extended further west during 2015, but it was fresher in the REF simulation compared to the SMOSexp experiment.

SSS data assimilation has also an impact on the other surface variables. SST differences at 5°N and velocity differences at the equator are represented on Fig. 14. The differences are mainly associated with the wave propagation seen in all the surface fields. In the freshwater pool, the SMOS data assimilation weakens the freshening and induces a slight warming of about 0.05°C (Fig14b). At the equator, there is an acceleration of the Warm Water Pool migration towards the east (Fig.14c) which helps the ocean-atmosphere coupling and thus the triggering of El Niño.

Fig. 15 shows the SSH evolution at 4°N during 2015. The left panels show the Sea Level Anomalies in the REF and SMOSexp simulations, the right panels being filtered at 33 days to highlight the TIW propagation, see (Yin et al., 2014; Lee et al., 2012) who show the capability of monitoring TIWs by Aquarius and SMOS data. A reinforcement of the TIWs (the slope is steeper) appears during the second half of 2015 in the SMOSexp experiment compared to the REF experiment. A similar result was found in (Hackert et al., 2014).

3.2 Evaluation of the analysis toward independent observations

We now compare the analysed fields to independent observations, i.e. withheld from all assimilation experiments. This will allow verifying that the changes in the physical fields induced by the SMOS data assimilation are in agreement with external sources of information. For this purpose, the TAO mooring (salinity) observations and the reprocessed TSG data from the French SS Observation Service were withheld from all experiments. This is therefore a fully independent validation.

3.2.1 Comparisons to TAO mooring

TAO moorings deliver high frequency measurements at fixed locations. Such platforms allow us to look at high frequency variability that is not captured by drifting platforms. The hourly analysed salinity is collocated at the TAO mooring positions for the REF and SMOSexp simulations. Fig. 16 shows the time evolution of TAO salinity observations (valid at 1 m depth) at three mooring locations in the equatorial Pacific (warm pool, cold tongue and salt front) compared to the model (analysis) for the REF and SMOSexp OSE experiments at the first level (~0.5 m depth). Assimilated SMOS data have also been added. In this example, the salinity evolution of the REF experiment (in green) appears less correlated with the TAO salinity mooring observations (black dots). The SMOSexp simulation shows a better agreement, except for some strongly variable events. The differences between the SMOSexp simulation and TAO non-assimilated observations are most of the time less than 0.1 PSU. The high frequency variability seen in the observations is also reproduced in the assimilative simulations, with a better agreement when SMOS data are assimilated, except during some specific periods. Tang et al., (2017) also found some disagreement between the TAO observations and SMAP/SMOS observations and Argo analysis during short periods. There is an improvement in the cold tongue during the end of summer, in fall 2015 and during the last 2 months of the SMOS simulation (16a) in the region where the data assimilation of SMOS reduces the freshening. Globally, an improvement occurs also in the warm pool (16b) over the entire period. One interesting feature is that when TAO mooring data are missing during a long

period near the salt front, the SSS from the SMOSexp experiment is different but closer to TAO mooring when measurements come back, Fig. 16c. Obviously, the assimilated 4-days SMOS data are smoother but are able to capture the large scale variability. This also shows the level of accuracy we need to capture higher variability. The precipitation rate superimposed on the SSS proves that it is not the only process that plays a role in the salinity variability. Indeed, a high precipitation rate does not induce necessarily a strong freshening at the sea surface where advection, vertical mixing and SSS SMOS data assimilation can counteract its effect. This also shows that the observation error should not be increased locally depending on the precipitation.

These three examples show a positive impact but it is also interesting to have a global view of all TAO moorings over the 2015/2016 El-Niño event.As in (Martin et al., 2018), Fig. 17 shows the differences in RMSD from hourly TAO mooring salinity values at 1 m depth calculated over the period 1st Jan 2015 to 16th March 2016. The impact of the SMOS assimilation is contrasted by showing positive (negative) values which indicates that it reduces (increases) the RMSD. The impact is positive and more significant in the West Tropical Pacific near the dateline and in the West Pacific up to 5°N. The impact is quite neutral and even negative in the East tropical Pacific (140°W-110°W) between 2°S and 2°N where generally (i) the SMOS bias is larger (Fig. 4b/5), (ii) there are few in-situ SSS data (Fig. 3) and (iii) where the observation error is larger (Fig. 7). Finaly, during the El-Niño 2015/2016 event, there is a small positive impact overall from the SMOS assimilation with a reduction in RMSD from 0.295 to 0.279 pss (about 5.5%).

3.2.1 Comparisons to ship SSS

Post processed TSG observations from the French SSS Observation Service SSS-OS) (http://www.legos.obs-mip.fr/observations/sss) were collected along the routes of voluntary merchant ships, see Alory et al., 2015. The SSS estimates have a ~2.5 km resolution along the ship track with an estimated error close to 0.08 pss. Salinity analysed fields from REF and SMOSexp simulations are collocated to the TSG observations. Salinity observations from vessel mounted thermosalinographs allow validation of the short time and space scales of near surface salinity. Two ship routes (Fig. 18) that cross the Tropical Pacific Ocean in June 2015 are chosen to verify that salinity changes when SSS SMOS data are assimilated are in agreement with such observations.

Fig. 19 shows the comparison between the TSG salinity observations (in red) along the Matisse ship route collocated with the REF (black dashed line) and SMOSexp (black line) salinity analyzed fields. The variability of the SSS measurements, lower than the daily frequency, is well represented in both simulations with only small differences of less than 0.2 PSU except in the freshwater on the eastern part of the basin. In this region, the salinity dropped down to less than 34.0 PSS. The REF simulation differs from the TSG data by more than 0.5 PSU within the freshwater pool, marked by a very sharp salinity front. The SMOSexp simulation shows a much better agreement with the SSS from the TSG observations: even if the differences remain large, the misfit is reduced.

This confirms once again that the weakening of the freshening in the freshwater pool in the eastern Pacific induced by the SMOS data assimilation is realistic, as it is seen by different in situ observation platforms.

Ocean Sci. Discuss., https://doi.org/10.5194/os-2018-113
Manuscript under review for journal Ocean Sci.
Discussion started: 22 October 2018

4. Discussion and conclusions

The L3 SMOS CATDS data used in this study is considered as an "unbiased" product. Yet, it still contains some residual biases that must be removed prior to data assimilation. It was the major challenge of this study: to estimate the residual SSS bias, and to estimate a suitable observation error for the system. It was made possible using an analysis of the residuals and errors with a statistical technique (Desroziers et al., 2005). Then the "debiased" data could be assimilated by the SAM2 assimilation scheme which relies on the unbiased hypothesis. The bias estimated by the ocean forecasting system can also be used to correct the L3 SMOS CATDS data for other purposes.

The system was carefully tuned and tested to efficiently assimilate the new SSS observations before running the longer simulations that are analyzed here. The proper specification of the observation operator and error covariance matrix were also based on discussions with the data provider. This study helped us to progress in the understanding of the biases and errors that can degrade the SMOS SSS performance.

There is still room for improvement. For instance, we used a zonal error as input to the error estimation with the Dezroziers technique. It could be beneficial to take into account the smaller scales linked to a shallow stratification that arises with strong precipitations or river runoff.

The SMOS data need in situ data to correct their own biases and estimate a suitable error (including data/system representativity). When enough data is available, SMOS really acts as a gap filler. There is a clear impact on the scales about 1°-2°. This can be seen on the Fig. 14 and Fig. 15 (Hovmuller), and additional spectral analyses (not shown) confirm this finding. So, it is important for future satellite SSS to provide a good accuracy in this band. It also shows that background error correlation length-scales used in the bias correction scheme could be optimized by improving the in-situ network and the SSS SMOS accuracy.

The focus of this study was on the tropical Pacific. But the system is global, and, in spite of RFI pollution near some coasts, we found clear improvements near the Amazon, Rio Del Plata, … So, the benefit from assimilating SMOS SSS is not restricted to the equatorial band. Its positive impact near the mid-latitudes major rivers is a chance to better monitor the strengthening of the water cycle (Durack, 2015).

Globally, SSS data assimilation slightly improves the simulation compared to already assimilated observations of in situ, SST and SLA data. It highlights that no incoherent information was brought by the SSS data compared to the other assimilated observations. When looking at the impact of the SMOS SSS assimilation, we found a positive impact in salinity over the top 30 meters. There is little impact on the SST. For instance, the area of the SST warmer than 28.5°C was little affected. It means that the local impact on the air-sea coupling is negligible. But we did find impact on the TIWs that were reinforced by acting on the SSH. The Barrier Layer Thickness was also impacted (not shown). The visible result can be seen on the strengthened Eastward advection of the warm pool in 2015 (Fig. 15**,** Hovmuller of zonal velocity difference). It means that SMOS SSS

assimilation has a non-local impact on the ocean-atmosphere dynamics. These findings are close to those of (Hackert et al., 2014) with a global ocean-atmosphere coupled model. Benefits in term of seasonal forecasting have still to be quantified. The next step will be to assimilate SSS from space at higher latitudes where low sea surface temperature (SST) degrades the brightness temperature sensitivity to SSS (Sabia et al., 2014). A longer ocean reanalysis with continuously improved SSS SMOS (available for over 9 years) and SMAP (available since 2015) data could bring new information on the water cycle.

Acknowledgements

We gratefully acknowledge funding from ESA as part of the SMOS-Niño15 project, coordinated by C. Donlon. We also thank the providers of the datasets used here. J. Boutin (LOCEAN/CATDS) provided the SMOS data and provided useful inputs to understand the nature of the SMOS bias estimates. Sea surface salinity data derived from voluntary observing ships were collected, validated, archived, and made freely available by the French Sea Surface Salinity Observation Service (http://www.legos.obs-mip.fr/observations/sss/). Thanks to the GTMBA Project Office of NOAA/PMEL to provide TAO/TRITON mooring data. We would also like to acknowledge Matthew Martin (MetOffice) for his careful reading of the manuscript and his comments which were very helpful.

References

Alory, G., Delcroix, T., Téchiné, P., Diverrès, D., Varillon, D., Cravatte, S., Gouriou, Y., Grelet, J., Jacquin, S., Kestenare, E., Maes, C., Morrow, R., Perrier, J., Reverdin, G., Roubaud, F., The French contribution to the voluntary observing ships network of sea surface salinity. Deep-Sea Res. 105, 1–18. http://dx.doi.org/10.1016/j.DSR.2015.08.005, 2015.

Ashok, K., and T. Yamagata, The El Niño with a difference. Nature. 461, 481-484, 2009.

Benkiran, M. and E. Greiner , Impact of the Incremental Analysis Updates on a Real-Time System of the North Atlantic Ocean. Journal of Atmospheric and Oceanic Technology 25(11): 2055-2073, 2008.

Bloom, S. C., L. L. Takacs, A. M. da Silva, and D. Ledvina, Data assimilation using incremental analysis updates. Mon. Wea. Rev., 124, 1256–1271, https://doi.org/10.1175/1520-0493(1996)124<1256:DAUIAU>2.0.CO;2, 1996.

Boutin, J., Vergely, J.L., Marchand, S., SMOS SSS L3 Debias v2 Maps Generated by CATDS CEC LOCEAN. http://dx.doi.org/10.17882/52804, 2017.

Boutin, J., Chao, Y., Asher, W. E., Delcroix, T., Drucker, R., Drushka, K., et al. . Satellite and In Situ Salinity: Understanding Near-Surface Stratification and Subfootprint Variability. Bulletin of the American Meteorological Society, 97(8), 1391–1407. https://doi.org/10.1175/BAMS-D-15-00032.1, 2016.

Chakraborty, A., R. Sharma, R. Kumar, and S. Basu, A SEEK filter assimilation of sea surface salinity from Aquarius in an OGCM: Implication for surface dynamics and thermohaline structure, J. Geophys. Res. Oceans, 119, doi:10.1002/2014JC009984, 2014.

Corbett, C. M., Subrahmanyam, B., & Giese, B. S., A comparison of sea surface salinity in the equatorial Pacific Ocean during the 1997–1998, 2012–2013, and 2014–2015 ENSO events. Climate Dynamics, 3513–3526. https://doi.org/10.1007/s00382-017-3527-y., 2017.

Dai, A. and Trenberth, K. E.: Estimates of freshwater discharge from continents: latitudinal and seasonal variations, J. Hydrometeorol., 3, 660–687, 2002.

Dai A., Qian, T., Trenberth, K., and Milliman, J. D.: Changes in Continental Freshwater 31 Discharge from 1948 to 2004, J. Climate, vol. 22, p.2773-2792, 2009.

Desroziers,G., L. Berre, B. Chapnik, and P. Poli. Diagnosis of observation, background and analysis error statistics in observation space. Quarterly Journal of the Royal Meteorological Society, 131:3385–3396, 2005.

Durack, P.J. Ocean salinity and the global water cycle. Oceanography 28(1):20–31, https://doi.org/10.5670/oceanog.2015.03., 2015.

Gasparin, F., and D. Roemmich, The strong freshwater anomaly during the onset of the 2015/2016 El Niño, Geophys. Res. Lett., 43, 6452–6460, doi:10.1002/2016GL069542, 2016.

Guimbard, S., Reul, N., Chapron, B., Umbert, M., & Maes, C., Seasonal and interannual variability of the Eastern Tropical Pacific Fresh Pool. Journal of Geophysical Research: Oceans, 122, 1749–1771. https://doi.org/10.1002/2016JC012130, 2017.

Good, S. A., M. J. Martin, and N. A. Rayner (2013), EN4: Quality controlled ocean temperature and salinity profiles and monthly objective analyses with uncertainty estimates, J. Geophys. Res. Oceans, 118, 6704–6716, doi:10.1002/2013JC009067.

Hackert, E., Busalacchi, A. J., & Ballabrera-Poy, J., Impact of Aquarius sea surface salinity observations on coupled forecasts for the tropical Indo-Pacific Ocean. Journal of Geophysical Research: Oceans, 119, 4045–4067. https://doi.org/10.1002/2013JC009697, 2014.

Hasson, A., Puy, M., Boutin, J., Guilyardi, E., Morrow, R., Northward propagation across the tropical North Pacific Ocean revealed by surface salinity: how El Nino anomalies reach Hawaii? J. Geophys. Res. 123. http://dx.doi.org/10.1002/2017JC013423, 2018.

Kidd, C., Dawkins, E., and Huffman, G.: Comparison of precipitation derived from the ECMWF operational forecast model and satellite precipitation datasets, J. Hydrometeorol., 14, 1463–1482, doi:10.1175/JHM-D-12-0182.1, 2013.

Köhl A, Sena Martins M, Stammer D., Impact of assimilating surface salinity from SMOS on ocean circulation estimates. J. Geophys. Res.-Oceans, 119, 5449-5464, doi: 10.1002/2014JC010040, 2014.

Lellouche, J.-M., Le Galloudec, O., Drévillon, M., Régnier, C., Greiner, E., Garric, G., Ferry, N., Desportes, C., Testut, C.-E., Bricaud, C., Bourdallé-Badie, R., Tranchant, B., Benkiran, M., Drillet, Y., Daudin, A., and De Nicola, C.: Evaluation of global monitoring and forecasting systems at Mercator Océan, Ocean Sci., 9, 57–81, doi:10.5194/os-9-57-2013, 2013.

Lellouche, J.-M., Greiner, E., Le Galloudec, O., Garric, G., Regnier, C., Drevillon, M., Benkiran, M., Testut, C.-E., Bourdalle-Badie, R., Gasparin, F., Hernandez, O., Levier, B., Drillet, Y., Remy, E., and Le Traon, P.-Y.: Recent updates on the Copernicus Marine Service global ocean monitoring and forecasting real-time 1/12° high resolution system, Ocean Sci., 14, 1093-1126, https://doi.org/10.5194/os-14-1093-2018, 2018.

Lahoz, W., Khattatov, B., Menard, R. (Eds.), Data assimilation: Making Sense of Observation, Springer Berlin Heidelberg, DOI 10.1007/978-3-540-74703-1, 2010.

Lee,T., G. Lagerloef, M. M. Gierach, H.-Y. Kao, S. Yueh, K. Dohan, Tropical instability waves linked to sea surface salinity anomalies,vol39, issue 12, DOI:10.1029/2012GL052232, 2012.

Lea, D. J., Martin, M. J. and Oke, P. R., Demonstrating the complementarity of observations in an operational ocean forecasting system. Q.J.R. Meteorol. Soc., 140: 2037-2049. doi: 10.1002/qj.2281, 2014.

Madec G.. NEMO Ocean Engine, Tech. Rep. 27, Pole de modelisation de IPSL, http://www.nemo-ocean.eu/About-NEMO/Reference-manuals/NEMO_book_3.6_STABLE., 2016.

McPhaden, M. J., Timmermann, A., Widlansky, M. J., Balmaseda, M. A., & Stockdale, T. N., The curious case of the El Niño that never happened: A perspective from 40 years of progress in climate research and forecasting. Bulletin of the American Meteorological Society, 96(10), 1647–1665, 2015.

Martin M. J., , R. R. King, J. While and A. Aguiar, Assimilating satellite sea surface salinity data from SMOS, Aquarius and SMAP into a global ocean forecasting system, submitted to QJRMS, 2018.

Oke, P.R., G. Larnicol, Y. Fujii, G.C. Smith, D.J. Lea, S. Guinehut, E. Remy, M. Alonso Balmaseda, T. Rykova, D. Surcel-Colan, M.J. Martin, A.A. Sellar, S. Mulet & V. Turpin, Assessing the impact of observations on ocean forecasts and reanalyses: Part 1, Global studies, Journal of Operational Oceanography, 8:sup1, s49-s62, 2015.

Oke, P.R., G. Larnicol, E.M. Jones, V. Kourafalou, A.K. Sperrevik, F. Carse, C.A.S. Tanajura, B. Mourre, M. Tonani, G.B. Brassington, M. Le Henaff, G.R. Halliwell Jr., R. Atlas, A.M. Moore, C.A. Edwards, M.J. Martin, A.A. Sellar, A. Alvarez, P. De Mey & M. Iskandarani, Assessing the impact of observations on ocean forecasts and reanalyses: Part 2, Regional applications, Journal of Operational Oceanography, 8:sup1, s63-s79, 2015.

Oke, P. R., Brassington, G. B., Griffin, D. A., and Schiller, A.: The Bluelink Ocean Data Assimilation System (BODAS), Ocean Model., 21, 46–70, 2008.

Reul N., Fournier S., Boutin J., Hernandez O., Maes C., Chapron B., Alory G., Quilfen Y., Tenerelli J., Morisset S., Kerr Y., Mecklenburg S.and Steven Delwart, Sea Surface Salinity Observations from Space with the SMOS Satellite: A New Means to Monitor the Marine Branch of the Water Cycle, Surveys in Geophysics, p 1-42, DOI: 10.1007/s10712-013-9244-0, http://link.springer.com/article/10.1007%2Fs10712-013-9244-0, 2013.

Sabia, R., A. Cristo, M. Talone, D. Fernández-Prieto and M. Portabella, "Impact of Sea Surface Temperature and Measurement Sampling on the SMOS Level 3 Salinity Products," in IEEE Geoscience and Remote Sensing Letters, vol. 11, no. 7, pp. 1245-1249, doi: 10.1109/LGRS.2013.2290710, 2014.

Seelanki V, Sreenivas P, Prasad KVSR. Impact of Aquarius Sea-Surface Salinity Assimilation in Improving the Ocean Analysis Over Indian Ocean. Marine Geodesy, 41 (2), 144-158, doi: 10.1080/01490419.2017.1422817., 2018.

Tang, Wenqing; Fore, Alexander; Yueh, Simon; Lee, Tong; Hayashi, Akiko; Sanchez-Franks, Alejandra; Martinez, Justino; King, Brian; Baranowski, Dariusz., Validating SMAP SSS with in situ measurements. Remote Sensing of Environment, 200. 326-340. https://doi.org/10.1016/j.rse.2017.08.021, 2017.

Toyoda T, Fujii Y, Kuragano T, Matthews JP, Abe H, Ebuchi N, Usui N, Ogawa K, Kamachi M., Improvements to a Global Ocean Data Assimilation System Through the Incorporation of Aquarius Surface Salinity Data. Q. J. Roy. Meteor. Soc., 141 (692), 2750-2759, doi: 10.1002/qj.2561., 2015.

Tranchant, B., Greiner, E., legalloudec, O. And Letraon P.: Sea Surface Salinity Data Assimilation Improvement in a Global Ocean Forecasting System at 1/4° from SMOS and Aquarius Data, 2nd science SMOS conference, 25-29 May 2015, ESA-ESAC, (near Madrid) Spain, 2015.

Von Schuckmann et al., The Copernicus Marine Service Ocean State Report, Journal of Operational Oceanography, https://doi.org/10.1080/1755876X.2018.1489208, 2018.

Yin, X., J. Boutin, G. Reverdin, T. Lee, S. Arnault, and N. Martin, SMOS Sea Surface Salinity signals of tropical instability waves, J. Geophys. Res. Oceans, 119, 7811–7826, doi:10.1002/2014JC009960, 2014.

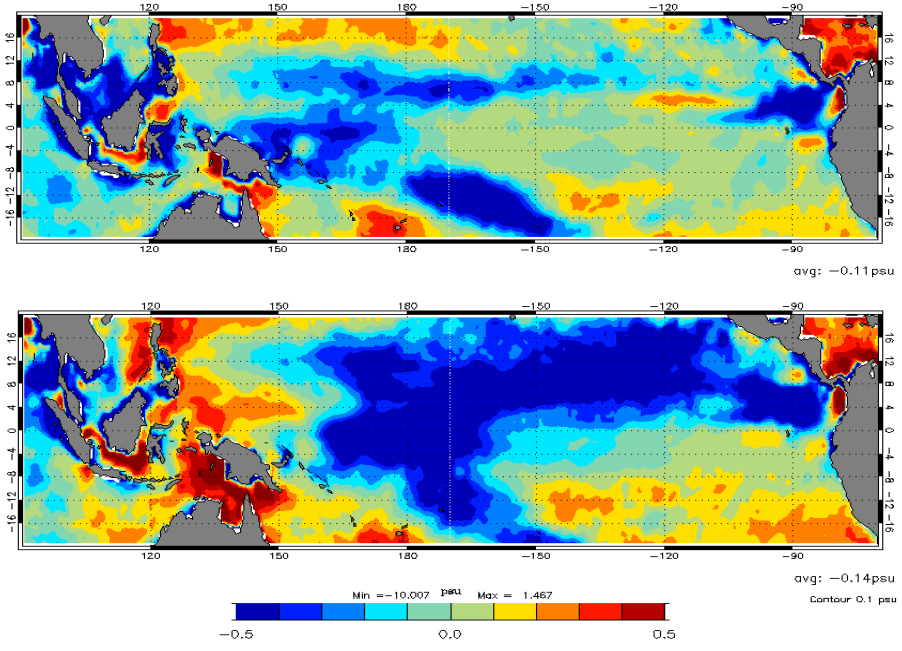

Ocean Sci. Discuss., https://doi.org/10.5194/os-2018-113
Manuscript under review for journal Ocean Sci.
Discussion started: 22 October 2018

Ocean Science
Discussions
Open Access
EGU

Figure 1: SSS anomalies (pss) in 2014 (top) and 2015 (bottom): mean salinity difference (model (control run) – WOA2013).

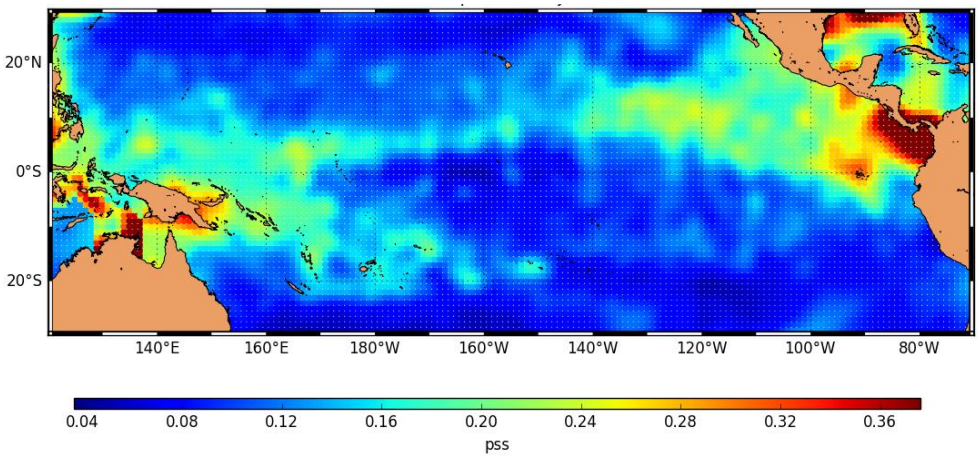

Figure 2: Representativity error of in-situ SSS ($R_{repr.}$) over the Tropical Pacific used in the data assimilation system.

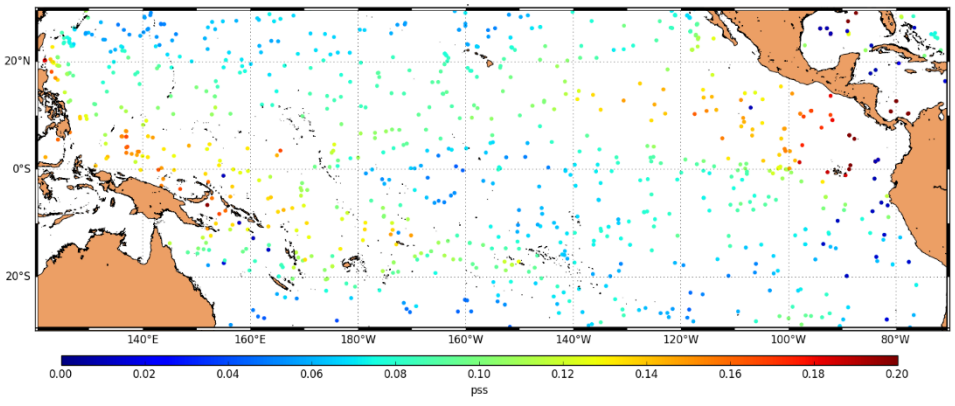

Figure 3: Example of salinity error of in-situ data at sea surface over the Tropical Pacific and used in the data assimilation system for the week 20-27 January 2016.

Ocean Sci. Discuss., https://doi.org/10.5194/os-2018-113
Manuscript under review for journal Ocean Sci.
Discussion started: 22 October 2018

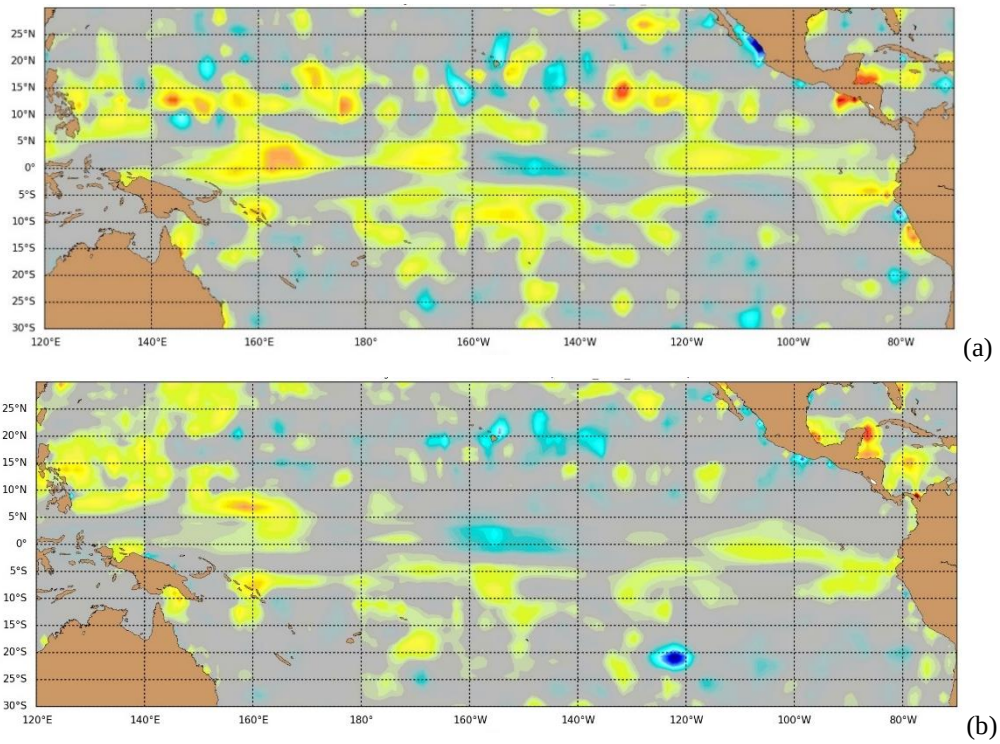

Figure 4: Example of model salinity bias near the surface (x, see Eq. 1a) calculated with the bias correction scheme inferred from in-situ data between 0 and 10 m depth only (a) and with the SSS term (ξ, see Eq. 1b) from SMOS data (b) averaged over 1 month in the Tropical Pacific (week 20-27 January 2016).

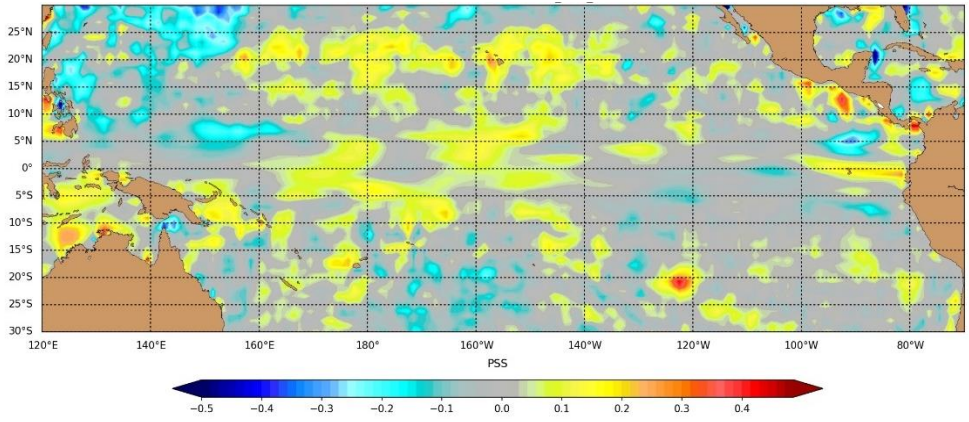

Figure 5: Example of SSS bias ξ calculated with the bias correction scheme inferred from in-situ data between 0 and 10 m and SMOS SSS averaged over 1 month in the Tropical Pacific (week 20-27 January 2016).

Ocean Sci. Discuss., https://doi.org/10.5194/os-2018-113
Manuscript under review for journal Ocean Sci.
Discussion started: 22 October 2018

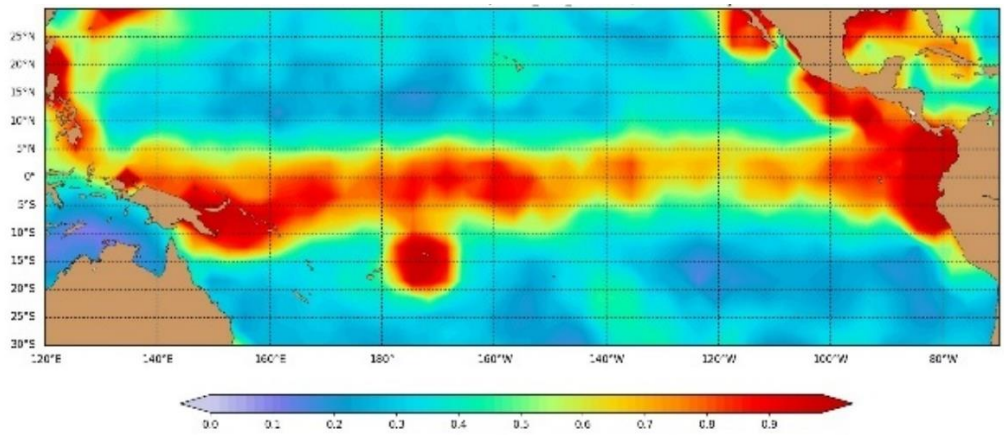

Figure 6: Example of Desroziers ratio (3°X3°) (see Eq. 3) estimated and applied to the a-priori error (bottom). (week 20-27 January 2016)

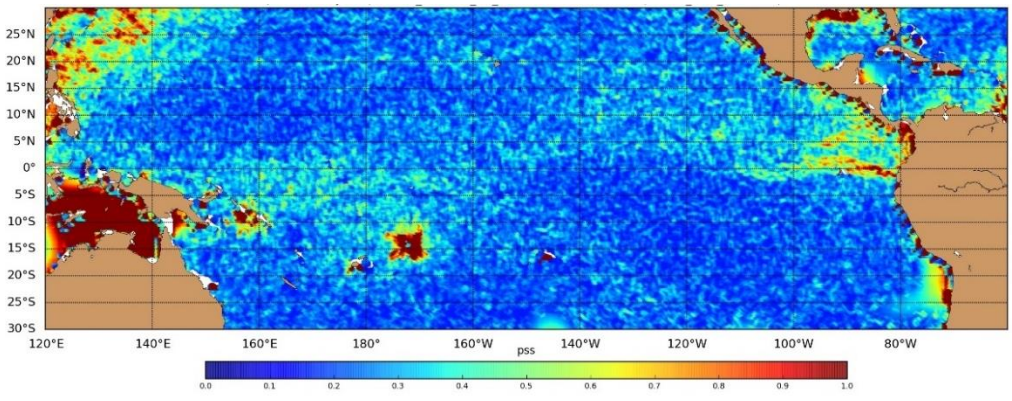

Figure 7: Example of SSS error (Eq. 4) of SMOS over the Tropical Pacific and used in the data assimilation system for the week 20-27 January 2016.

Ocean Sci. Discuss., https://doi.org/10.5194/os-2018-113
Manuscript under review for journal Ocean Sci.
Discussion started: 22 October 2018

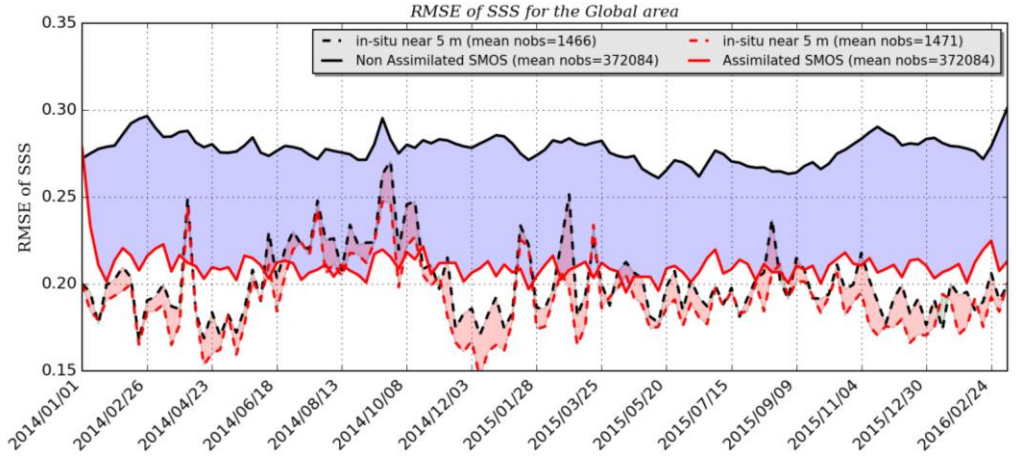

(a)

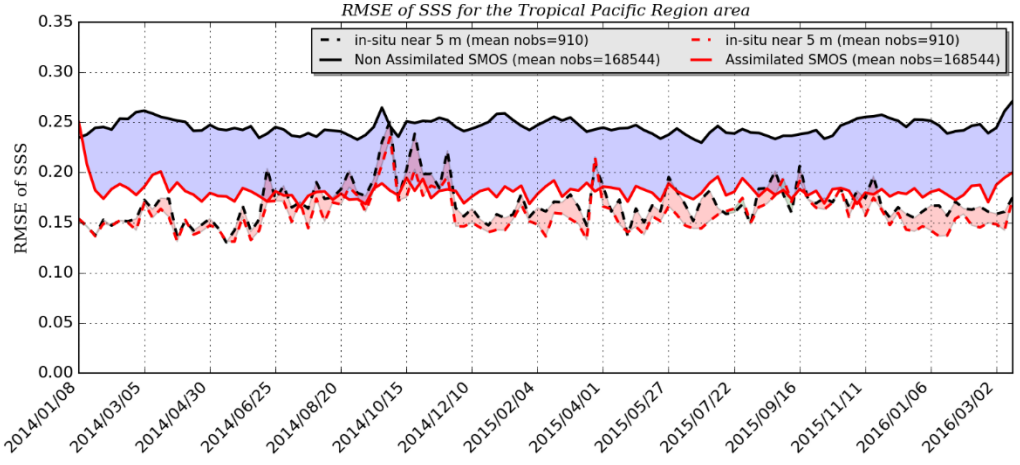

(b)

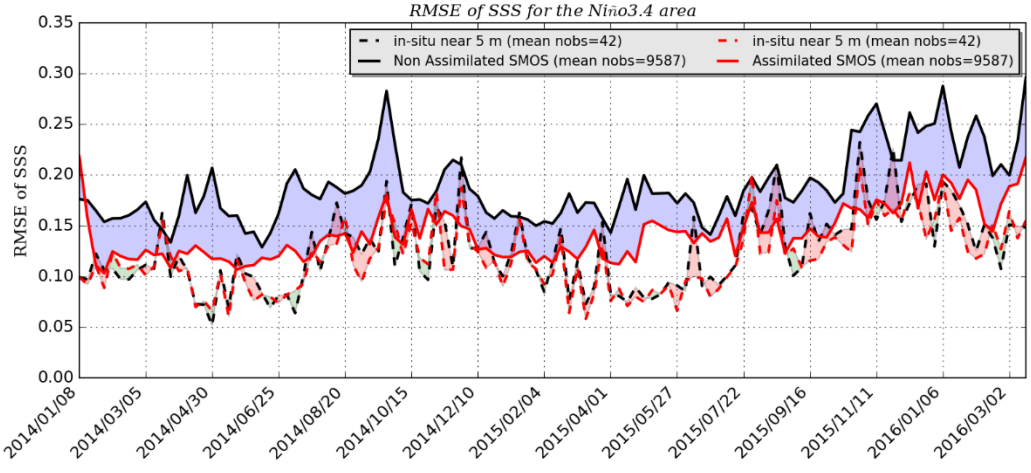

(c)

Ocean Sci. Discuss., https://doi.org/10.5194/os-2018-113
Manuscript under review for journal Ocean Sci.
Discussion started: 22 October 2018

Figure 8: RMSE of SMOS SSS and in situ salinity observations near 5 meter depth, for the reference simulation (solid line) and the SMOSexp simulation (dashed line), over the global domain (top), over the Tropical Pacific (middle) and in the Niño3.4 region (bottom). The mean number (weekly) of observations are mentionned.

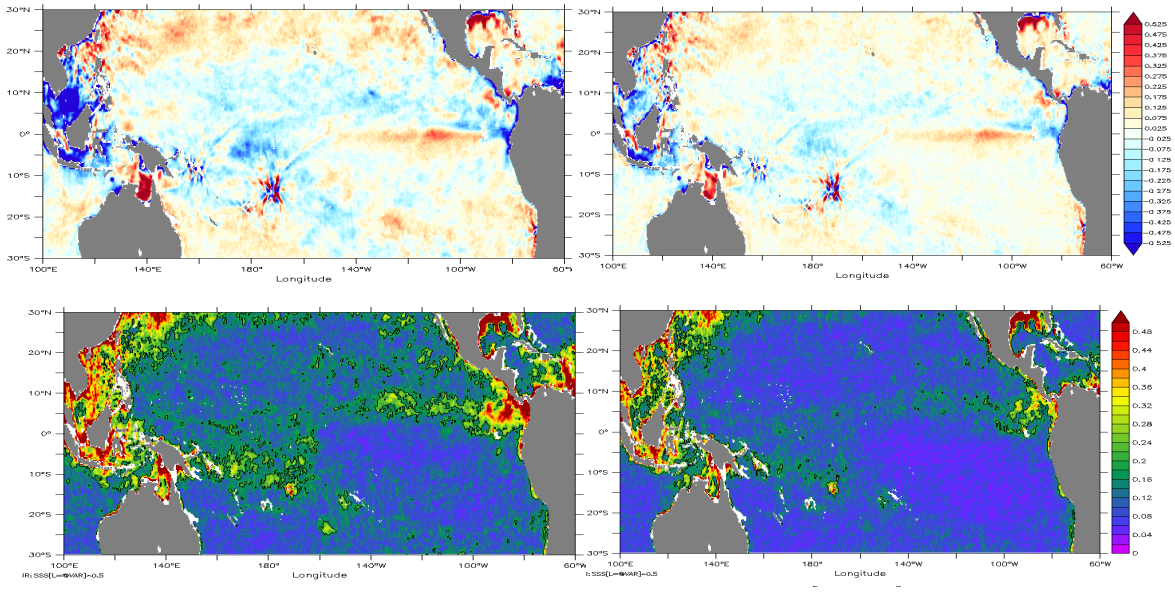

Figure 9: Statistics (from daily mean) mean (top) and standard deviation (bottom) of SSS difference (model -SMOS observation) for REF (left) and SMOSexp (right) experiments on 2015 year.

Ocean Sci. Discuss., https://doi.org/10.5194/os-2018-113
Manuscript under review for journal Ocean Sci.
Discussion started: 22 October 2018

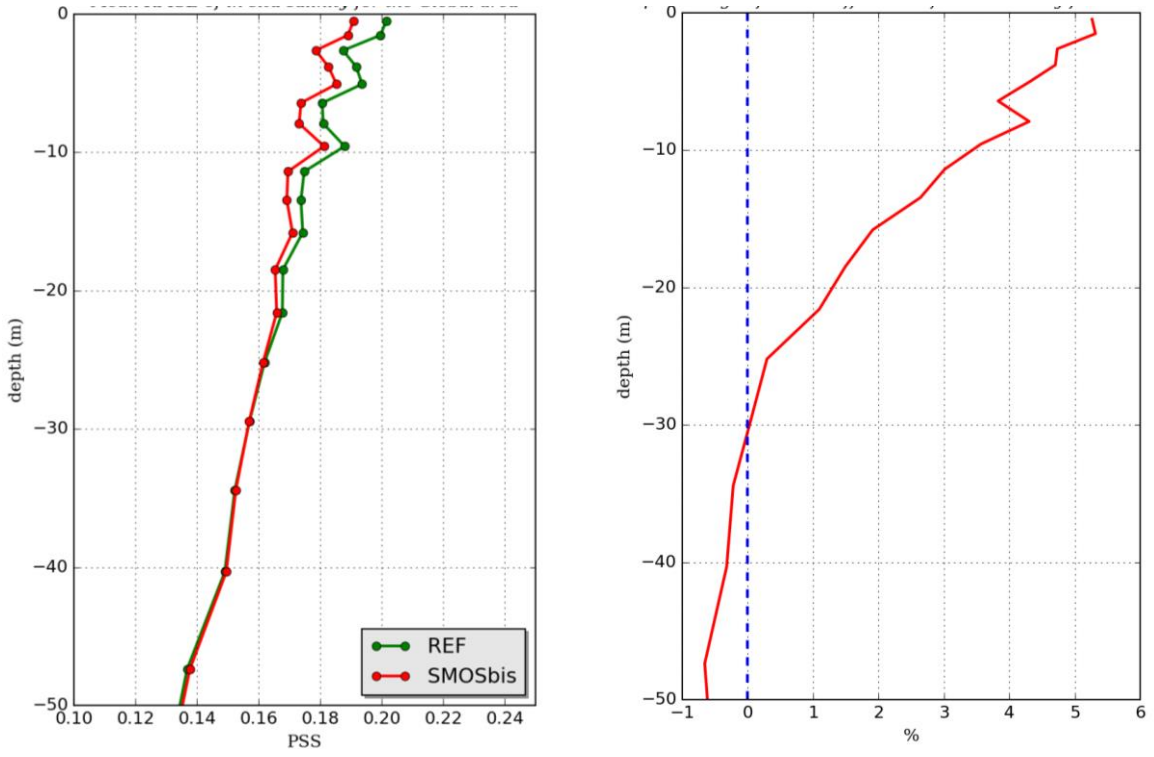

Figure 10: Average salinity RMSE (pss) compared to all in situ measurements (left) over the period 1st Jan 2014 to 2st Mar 2016 in global domain for the *REF* (green line) and *SMOSexp* (red line) experiments as a function of depth over the top 50 m. The corresponding percentage of RMSE difference of all in situ salinity measurements between REF and SMOSexp experiments (right) (positive difference implies a reduction in RMSE by the SSS assimilation).

5

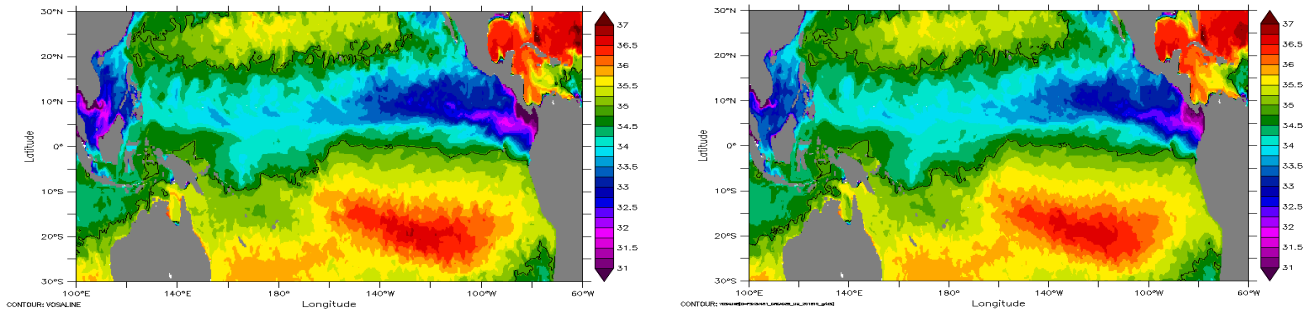

Ocean Sci. Discuss., https://doi.org/10.5194/os-2018-113
Manuscript under review for journal Ocean Sci.
Discussion started: 22 October 2018

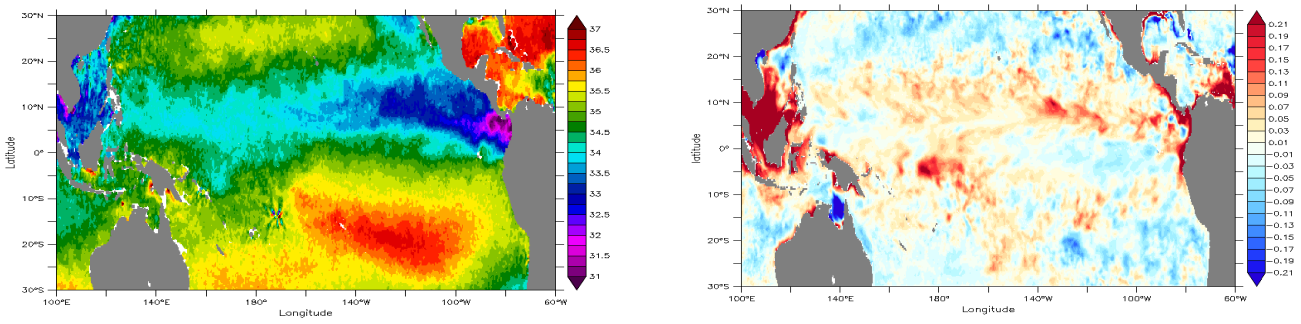

Figure 11: Mean October 2015 SSS estimation from the REF experiment (top, left), the SMOSexp experiment (top, right), the SMOS SSS measurements (left, bottom) and annual mean difference (2015) between the SMOSexp and REF experiment (bottom, right).

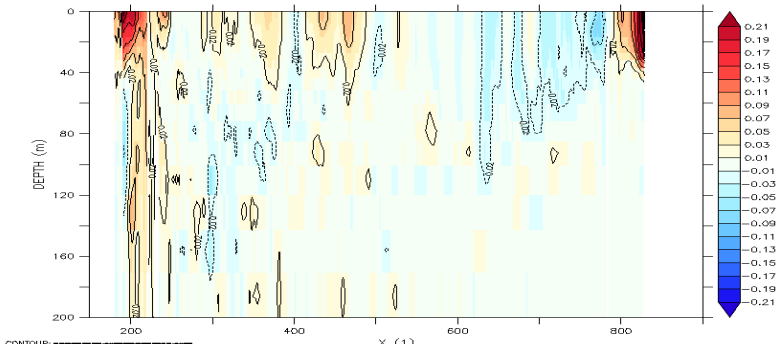

Figure 12: Vertical section along the equator of the mean model salinity difference between the SMOSexp and REF experiments for the year 2015.

Ocean Sci. Discuss., https://doi.org/10.5194/os-2018-113
Manuscript under review for journal Ocean Sci.
Discussion started: 22 October 2018

Ocean Science
Discussions
Open Access
EGU

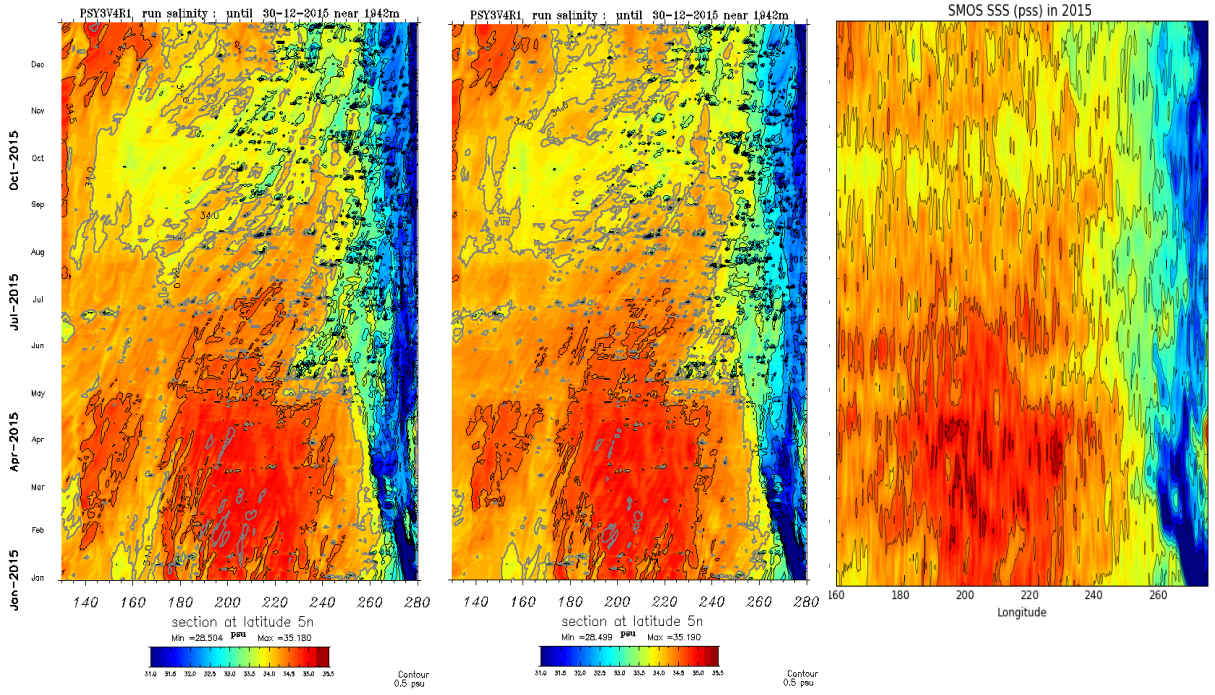

Figure 13: Hoevmuller of SSS at 5°N for the REF (left) and SMOSexp (middle) and SMOS data (right)

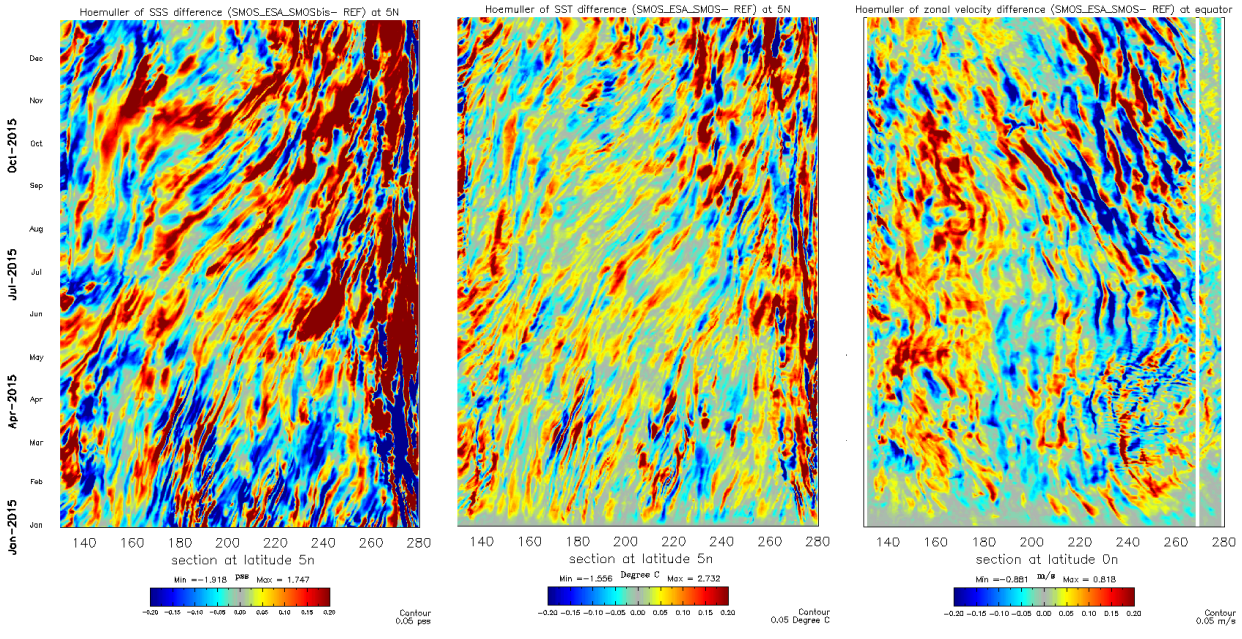

Figure 14: Hoevmuller ofdifferences in SSS (left), SST(middle) at 5°N and sea surface zonal velocity (U) (right) at the equator between the SMOSexp and the REF experiment in 2015.

Ocean Sci. Discuss., https://doi.org/10.5194/os-2018-113
Manuscript under review for journal Ocean Sci.
Discussion started: 22 October 2018

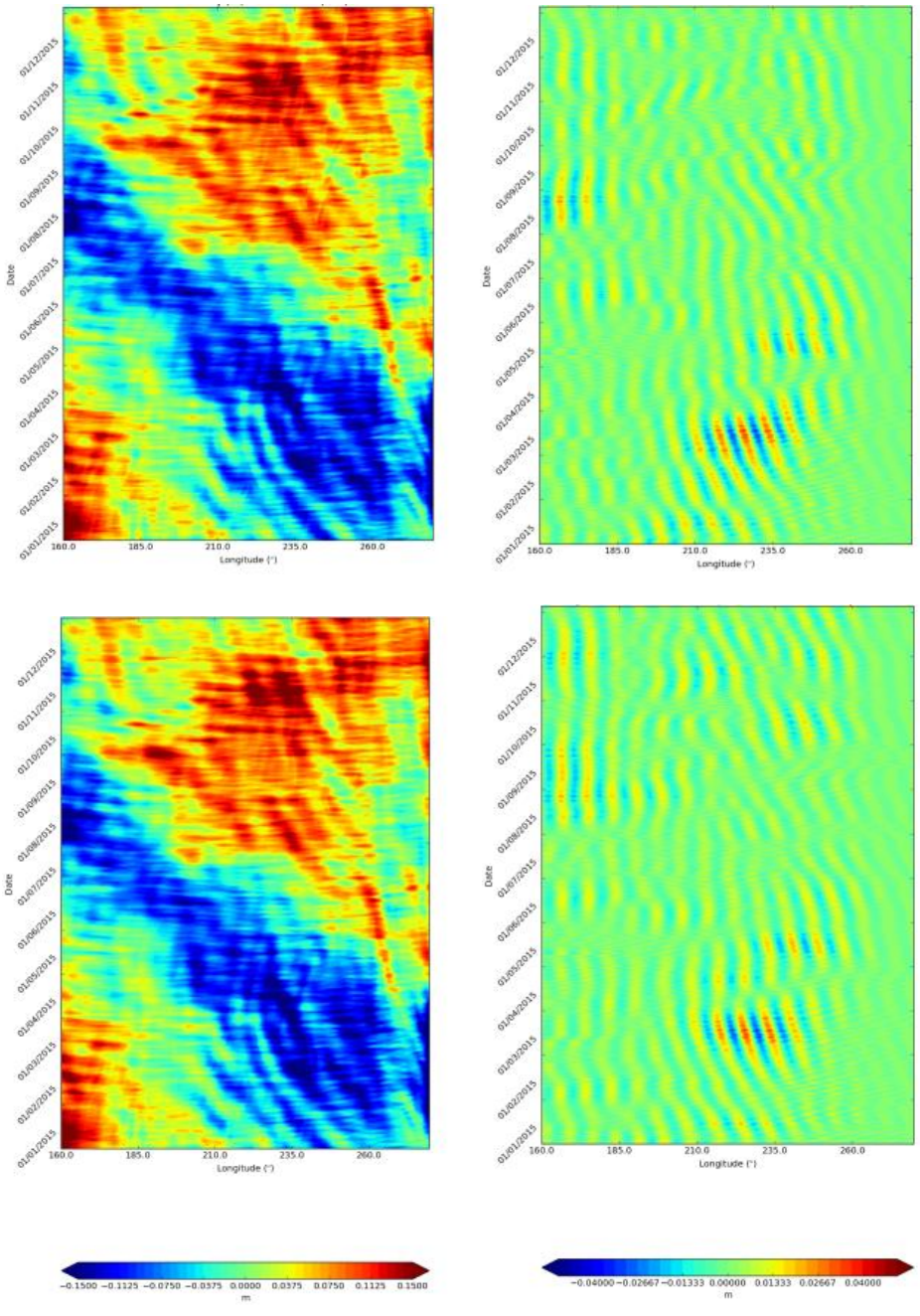

Figure 15: Hoevmuller of SSH (left) and filtered SSH (band-pass filter 28-40 days) at 4°N (right) for REF experiment (top) and for SMOSexp experiment (bottom) during 2015.

Ocean Sci. Discuss., https://doi.org/10.5194/os-2018-113
Manuscript under review for journal Ocean Sci.
Discussion started: 22 October 2018

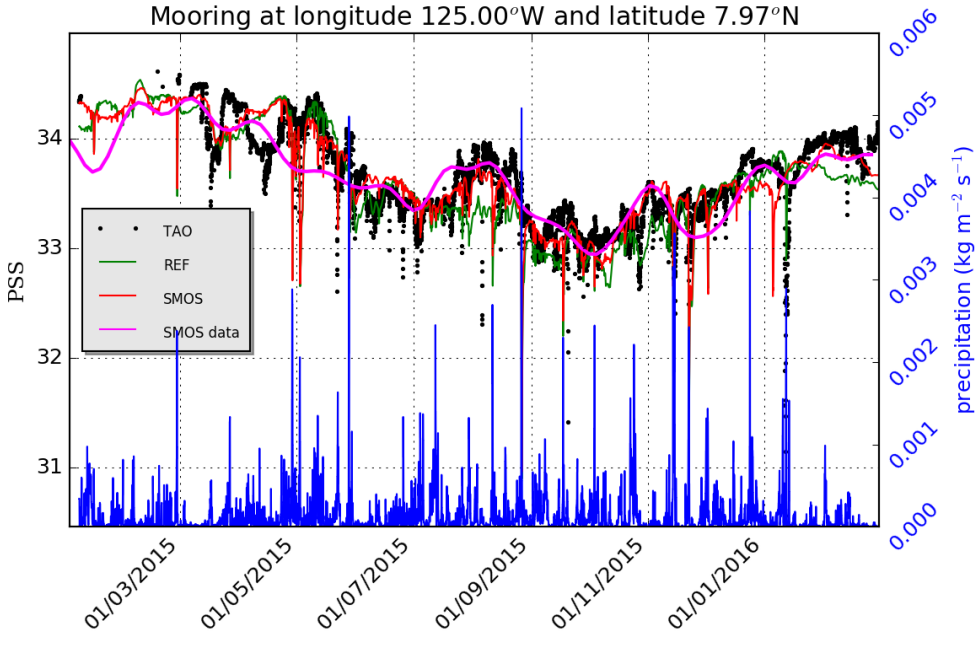

(a)

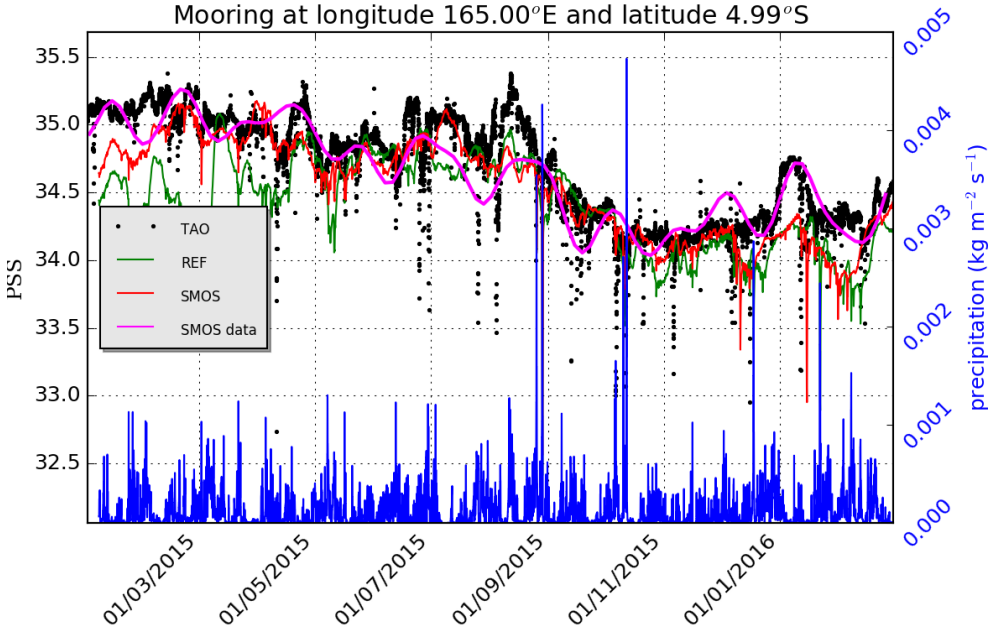

(b)

Ocean Sci. Discuss., https://doi.org/10.5194/os-2018-113
Manuscript under review for journal Ocean Sci.
Discussion started: 22 October 2018

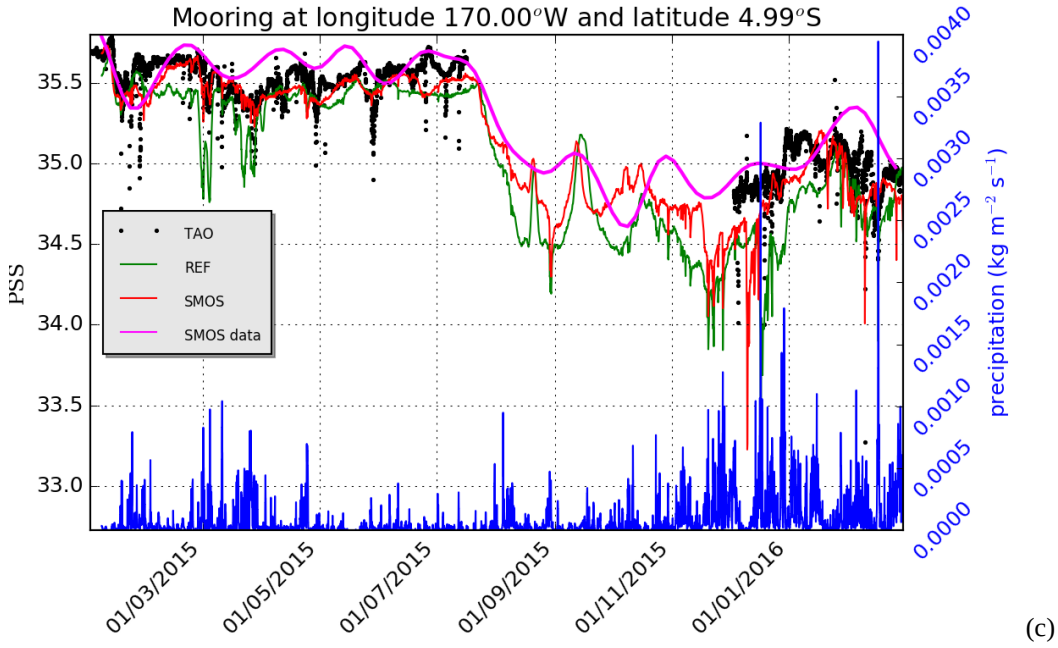

(c)

Figure 16: Time evolution of the hourly TAO observed salinity (black), the hourly model REF (green), SMOSexp (red) simulations and the assimilated SMOS data (magenta) at three different TAO moorings locations, cold tongue (a), warm pool (b) and (c) salt front (2015-March 2016). The precipitation rate (blue line) coming from the atmospheric ECMWF forcing is superimposed

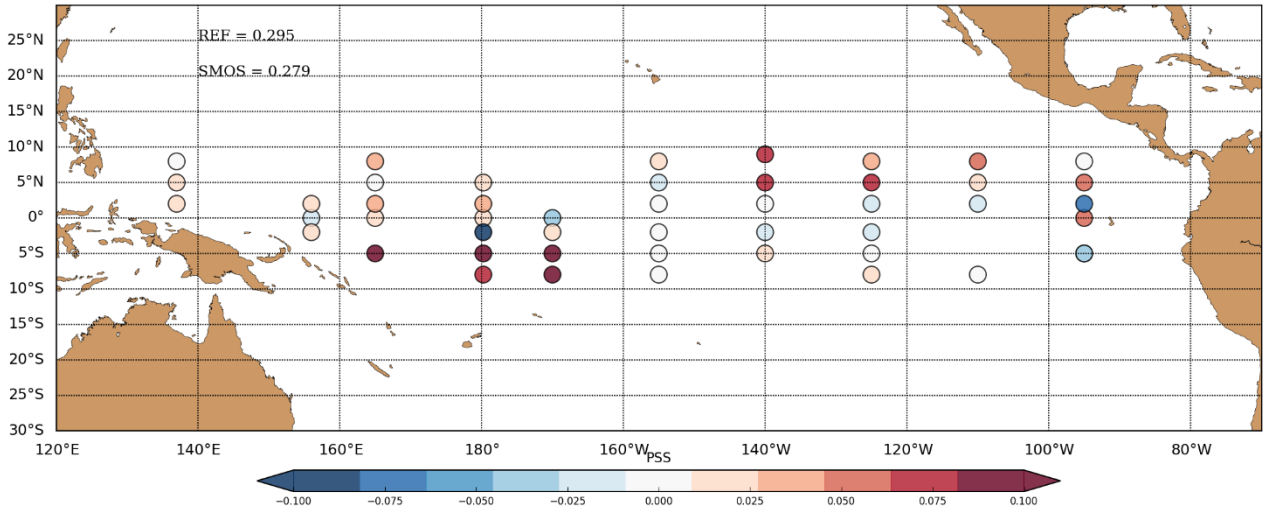

Figure 17. Difference in model salinity RMSD (pss) at 0.45 m depth calculated against the 1 m depth TAO mooring salinity values (*REF* – SMOSexp) calculated over the period 1st Jan 2015 to 16th March 2016 (positive/negative difference implies a reduction/increase in RMSD by the SMOS assimilation). Moorings are only included if they have more than 1 week of measurements during the period.

Ocean Sci. Discuss., https://doi.org/10.5194/os-2018-113
Manuscript under review for journal Ocean Sci.
Discussion started: 22 October 2018

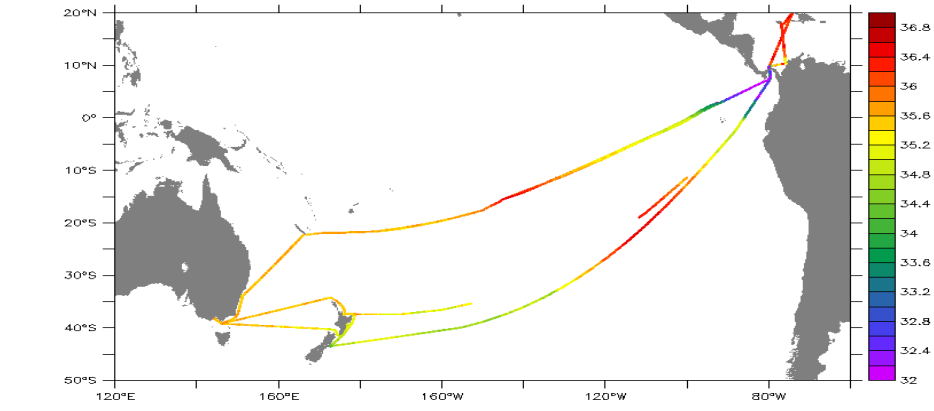

Figure 18: Ship routes with TSG salinity observations (PSS)

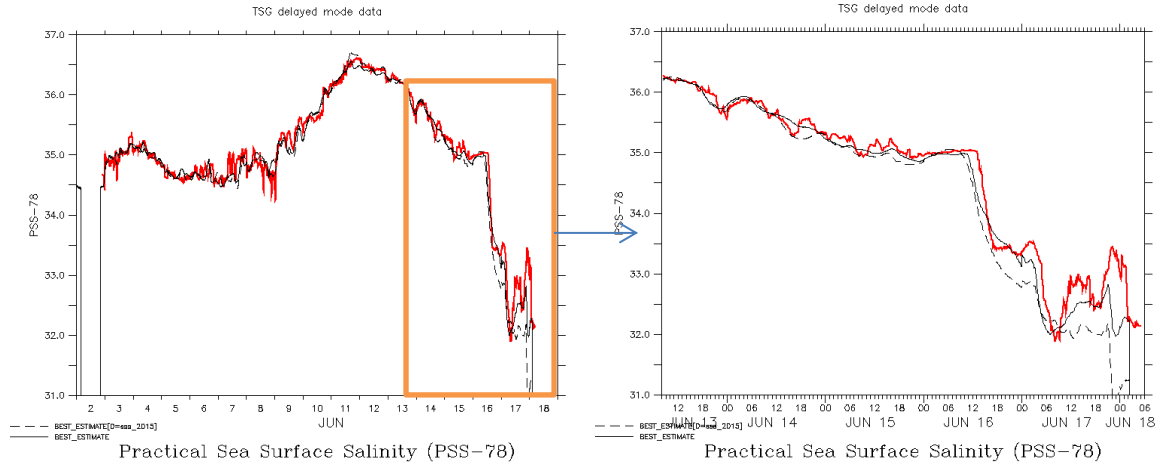

Figure 19: TSG Salinity observations and analysis from the OSEs along the Matisse ship track (LEGOS) (red = obs, dashed = REF, black line = SMOSexp).

Instrumental errors ($R_{inst.}$)	
Altimetry	
JASON2, ALTIKA/SARAL	2 cm
HAIYANG-2A	4 cm
SST	
OSTIA L4	0.5°C
In-situ at sea surface	
XBT, moorings, Argo floats, sea mammals	0.03°C and 0.0075 pss

Table 1: Instrumental errors used for the current operational network.

Ocean Sci. Discuss., https://doi.org/10.5194/os-2018-113
Manuscript under review for journal Ocean Sci.
Discussion started: 22 October 2018

Experiment name	Period	Assimilated observations	SSS product
Reference (REF) or control run	Jan 2014- March 2016	Current networks without satellite SSS.	No SSS assimilation
SMOSexp	Jan 2014 - March 2016	Current network plus SMOS satellite SSS observations.	4-day 0.25°x0.25° SMOS data from LOCEAN (L3-Debiased-Locean-v2)

Table 2: Experiment descriptions

region	Percentage of RMSE difference of SSS when SMOS SSS is assimilated and mean number of observations			
	SMOS SSS		In situ salinity at 5m	
	%	Mean number of obs.	%	Mean number of obs.
Global ocean	24 %	372,000	5 %	1500
Tropical Pacific	25%	168,500	6%	910
Niño 3.4	23%	9,900	4%	42
Niño 4 region	22 %	9,500	6 %	51
Niño 3	25%	11,400	1%	64
Niño 1+2 region	28 %	1,800	7 %	7

Table 3: Percentage of RMSE difference of SSS for SMOS and for in-situ salinity at 5 m depth in different regions. The mean number of assimilated SSS data are also shown.